

Highly localized heat generation by femtosecond laser induced plasmon excitation in Ag nanowires

Lei Liu, Peng Peng, Anming Hu, Guisheng Zou, W. W. Duley et al.

Citation: *Appl. Phys. Lett.* **102**, 073107 (2013); doi: 10.1063/1.4790189

View online: <http://dx.doi.org/10.1063/1.4790189>

View Table of Contents: <http://apl.aip.org/resource/1/APPLAB/v102/i7>

Published by the [American Institute of Physics](http://www.aip.org).

Additional information on *Appl. Phys. Lett.*



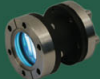



Journal Homepage: <http://apl.aip.org/>

Journal Information: http://apl.aip.org/about/about_the_journal

Top downloads: http://apl.aip.org/features/most_downloaded

Information for Authors: <http://apl.aip.org/authors>

ADVERTISEMENT

a sampling of our products		for surface and materials science	www. rbdinstruments .com	celebrating over 20 years of innovation
 deposition tools	 desorption systems	 sputter ion sources	 viewports	 usb picoammeters

Highly localized heat generation by femtosecond laser induced plasmon excitation in Ag nanowires

Lei Liu,^{1,2} Peng Peng,² Anming Hu,² Guisheng Zou,¹ W. W. Duley,³ and Y. Norman Zhou^{1,2}

¹Department of Mechanical Engineering, Tsinghua University, Beijing 100084, China

²Department of Mechanical and Mechatronics Engineering, University of Waterloo, Waterloo, Ontario N2L 3G1, Canada

³Department of Physics and Astronomy, University of Waterloo, Waterloo, Ontario N2L 3G1, Canada

(Received 7 August 2012; accepted 19 January 2013; published online 21 February 2013)

Photo-excitation of plasmons in nano-systems initially results in highly localized heating, but the final temperature distribution in irradiated nanostructures is almost uniform because heat diffusion equilibrates the overall temperature within $\sim 10^{-12}$ s. Here, we show that irradiation with femtosecond pulses enables visualization of the location of plasmonic heating because thermal effects such as plasmon-induced melting are frozen in at the initial location of energy deposition. Simulations show plasmonic heating is related to the orientation of the laser polarization and to the geometry of partially melted nanowires. This may provide a useful tool in joining, cutting, and reshaping nano-objects. © 2013 American Institute of Physics.

[<http://dx.doi.org/10.1063/1.4790189>]

The introduction of nano-heat sources induced by plasmonic effects are opening up a wide range of applications in microfluidics,^{1,2} medicine,^{3,4} welding,^{5,6} sub-wavelength laser,⁷ and imaging.^{8,9} Nano-devices based on the re-distribution of plasmonic energy can be constructed from nanoparticles, nanorods, nanowires (NWs), or complex nano-antennae.^{10,11} Since the time scale for thermal diffusion is typically $\sim 10^{-12}$ s in nanoscale systems, under continuous wave (CW) laser irradiation the temperature distribution inside a nano-device is essentially quasi-uniform, even though the plasmonic heat generation is highly spatially localized.^{12,13} This makes the location and distribution of plasmonic heat generation hard to observe experimentally. As a result, numerical simulation has become the primary tool used to characterize heating in thermoplasmonic systems.¹⁴ When compared to CW laser irradiation, femtosecond (fs) laser illumination initially constrains heat generation to thermal hot spots at spatial locations determined by the distribution of the plasmonic electric field in the object. This can induce large transient thermal gradients within nano-scale devices since, on a time scale of ~ 100 fs, heat generation and heat diffusion occur *successively*.^{14,15} Therefore, by using femtosecond laser pulses as an excitation source, the initial locations of heat deposition in nano-devices can be determined by observation of thermal effects such as melting and solidification which will be centered at the original sites of heat deposition.

In this paper, we use this method to determine the location of plasmonic heat deposition in Ag nanowires induced by a femtosecond laser. We find that some nanowires are melted over localized volumes at their ends and at regions where they cross other nanowires. Other nanowires do not show this localized melting. Selective melting and the location of this effect are found to be highly correlated to plasmonic heating induced by femtosecond laser pulses. Our observations, together with theoretical simulations, demonstrate that when the resonance wavelength of the nanowire matches the incident laser wavelength, melting tends to occur. The resulting distri-

bution of plasmon excitation is determined primarily by the dimensions of the nanowire and the polarization direction of the laser beam. However, we find that once melting occurs at the end of a nanowire, the nanowire then melts to produce several aligned nanoparticles. This process is the result of changes in the distribution of plasmon excitation accompanying the altered morphology. This method may be applicable to welding, cutting, and reshaping of nano-objects.

In our experiments, a Ti-sapphire laser system (Coherent, Inc.) was operated to generate 35 fs polarized laser pulses at repetition rate of 1 kHz and 800 nm with Gaussian beam distribution and laser fluence of 110 mJ/cm². The laser was elliptically polarized (10:1) and laser pulses were focused by a lens with a 13 cm focal length. A mechanical shutter was used to select the number of pulses per illumination. The Ag nanowires solution was drop-cast onto amorphous carbon coated (<50 nm in thickness) copper grid for femtosecond laser illumination in both air and vacuum (3.3×10^{-5} Torr). In order to check whether the carbon membrane substrate was influencing the results, a sample of nanowires in liquid was irradiated with fs laser pulses. The liquid was placed in a glass tube with 0.5 mm inner diameter and scanned at 1 mm/s with the same laser fluence.

Fig. 1(a) shows the typical morphology of nanowires on the amorphous carbon substrate after exposure to 8 fs laser pulses in air. It can be seen that the junction area between the two nanowires was melted and a cross wire nano-joint formed after irradiation. In addition, the ends of the nanowires melted to produce globe-like nano-structures with diameters ≈ 300 –500 nm. These structures remained attached to the ends of the nanowires. This suggests that a temperature gradient occurred toward the end of the wires during irradiation, as bulk heating of the wires with a hot plate in the absence of thermal gradients caused the nanowires to separate into large submicron/micron particles/rods as a result of surface tension.

Figs. 1(b) and 1(c) show bright and dark field TEM images of the extremity of a nanowire after plasmon-induced melting. It clearly indicates that the end of the nanowire

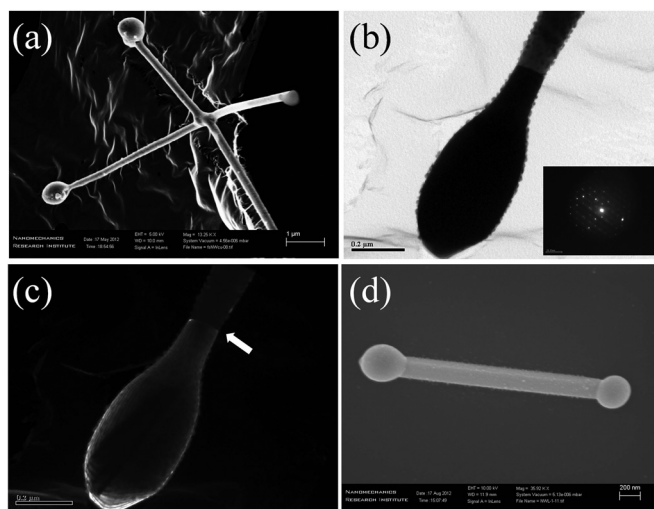


FIG. 1. Morphology of nanowires after femtosecond laser illumination indicating the location of plasmonic heating: (a)–(c) on an amorphous carbon substrate, (d) after irradiation in liquid. In (a) melting occurs at the ends of the nanowire and in the cross-sectional area adjacent to the junction between two wires. (b) and (c) Bright and dark field TEM images of the terminal nano-particles, showing a grain boundary caused by melting and solidification. (d) After irradiation in liquid without the presence of a substrate.

melted and then resolidified into a single crystalline Ag nanoparticle. A grain boundary can be seen in the connection between the melted end and the body of the nanowire, suggesting that the orientation of the melted extremity changed after laser illumination. This may be because the high solidification rate of the nanoparticle did not allow it to grow epitaxially from the original nanowire.¹⁶ It was also observed that some nanowires showed no melting after laser illumination, despite being exposed to the same laser fluence. In order to eliminate any influence of the amorphous carbon membrane substrate, a sample of nanowires was dispersed in water and irradiated with the same fluence without any substrate. Fig. 1(d) shows that the ends of the nanowires also melted under these conditions, indicating that the substrate did not play a role in the plasmonic localization process.

The absorption of laser pulse energy by silver nanowires can be described as a three-step process:^{14,15} electronic absorption, electron-phonon thermalization, and external heat diffusion. For fs laser pulses, these three steps occur sequentially.¹⁵ This implies that the heat absorption and heat diffusion processes are temporally separated and that thermal conductivity is essentially non-existent while heat is being introduced into the system. As a result, a large temperature gradient ($\sim 10^{11}$ – 10^{12} K/m) can exist in the nanowire on a transient basis when the heat source has non-uniform spatial distribution. This spatial non-uniformity arises as plasmons are created by the absorption of photons from the incident laser field. The propagation of these plasmons gives rise to the localization of plasmon energy at “hot-spots.” These are regions within the nano-structure where the field is enhanced, and heat dissipation is maximized. The localization of excitation within these hot-spots is the source of non-uniform heating and leads to the generation of thermal gradients.

From extensive work on coupled systems of nanowires, nanoparticles and films, as well as nanowires and nanoparticles, it is well established that highly localized plasmonic

fields can be generated in the junctions of these systems.⁵ The efficiency with which plasmon excitation is converted to heat within the junction area is related to the presence and configuration of the gaps between nanoobjects.⁵ Many studies have also demonstrated that the extremities of nanowires constitute hot spots, but the field intensity at these locations is much weaker than that existing at junctions or gaps.^{17,18} Melting at the cross junction areas by plasmonic heat has recently been directly observed,⁵ while melting at the end of nanowires has not been previously observed experimentally.

To understand the location of “hot spots” in relation to the resonance frequency of a single nanowire, finite difference time domain (FDTD) simulations were carried out using the Lumerical Solutions software package. Fig. 2(a) shows the melted end of a single isolated Ag nanowire after irradiation with 8 laser pulses in vacuum. The axis of the nanowire was oriented perpendicular to the direction of laser polarization. A 3D FDTD model based on the experimental result of Fig. 2(a) was developed to analyze this effect. To account for the actual shape of the fabricated nanowires, round corners with 42.5 nm radius were used.

Fig. 2(c) shows the calculated absorption spectrum of the nanowire in Fig. 2(a). The resonance wavelength of the nanowire was 780–800 nm, which was the same as the laser wavelength. As noted in the caption of Fig. 1, not every nanowire showed melting at its extremity. Our simulation for the melted nanowire indicates that once the resonance wavelength of the nanowire matches that of the incident laser, then melting tends to occur at the end of the wire. Fig. 2(d) shows the electric field distribution around the nanowire at its resonance wavelength, and confirms that the electric field is most intense at both ends of the wire. The field distribution along the sides of the nanowire is uniform. When quasi-spherical particles having a radius of ~ 150 nm form at the end of the nanowire (Fig. 2(e)), the electric field concentrates at the surface of these particles and they subsequently increase in volume. Due to this change in morphology, the electric field along the nanowire becomes non-uniform and is concentrated on the sides of the wire. Under these conditions, the absorption spectrum shifts to longer wavelength as the ends melt. The increased mass at each end of the nanowire and the non-uniform field distribution along the nanowire induce a tensile stress at the junction between the spherical mass and the wire, which eventually leads to separation at this point. The absorption spectrum does not change after separation and there is no additional concentration of the electric field after this occurs. Fig. 2(b) shows that the nanowire can, however, separate further into an array of nanoparticles.

With the direction of laser polarization is parallel to the long axis of the nanowire, the wire was observed to melt into several aligned nanoparticles or nanorods (Figs. 3(a) and 3(b)). Figs. 3(c)–3(f) show the FDTD simulation results for an Ag nanowire having the same dimension as that in Fig. 2(a) but excited with radiation having parallel polarization. The calculated absorption spectrum shown in Fig. 3(c) indicates that the nanowire has three resonance wavelengths between 600 and 1000 nm. Fig. 3(d) shows the electric field distribution around the nanowire at its 770 nm resonance and indicates that the strongest field confinement is located at the

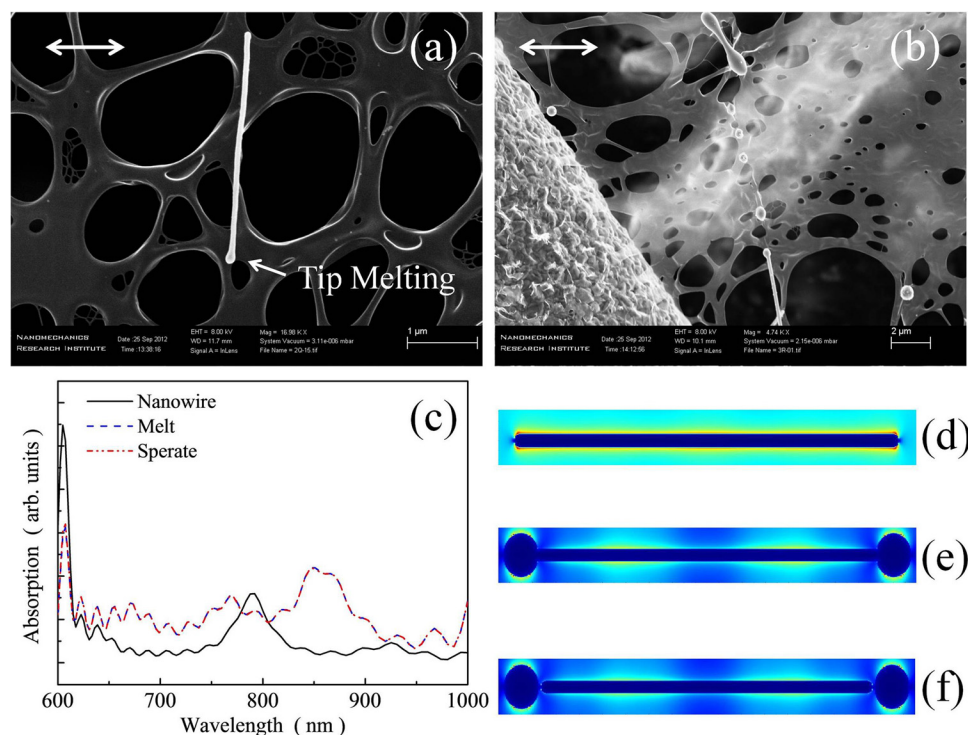


FIG. 2. Laser polarization perpendicular to the long axis of the Ag nanowire (a) melting at the end of the wire. (b) Distributed melting where the nanowire has separated into nanoparticles. (c) Absorption spectra as calculated from FDTD simulation. (d) Electric field $|E|$ distribution calculated by FDTD. (e) $|E|$ distribution when the Ag nanorod has melted at each end. (f) $|E|$ distribution when particles have separated from the end of the nanowire. The arrows indicate the polarization direction.

ends of the nanowire. Additional weaker modulations in the electric field along the sides of the nanowire are signatures of the multipolar resonance involved.¹⁷ These modulations enable one to assign the modes associated with resonances using the relation $L = (n + 1/2) \lambda_{\text{eff}}$, where L is the antenna length, λ_{eff} is the effective laser wavelength, and n is an integer.¹⁷ Using this result, the resonance of the isolated $3.3 \mu\text{m}$ nanowire at 770 nm is attributed to the $n=5$ mode with $\lambda_{\text{eff}} = 600 \text{ nm}$. When the multipolar resonance is sufficiently intense, irradiation with radiation polarized parallel to

the long axis of the nanowire can produce melting and the formation of an aligned array of Ag nanoparticles. This is obviously different from the results obtained on irradiation with perpendicularly polarized light (Fig. 2).

If the multipolar resonance is not strong enough to produce in melting within the nanowire, the ends of the nanowire are observed to melt forming globular structures. Fig. 3(e) shows the field distribution after these structures have formed. Under these conditions, weak modulations in the electric field are still present and the absorption spectrum has

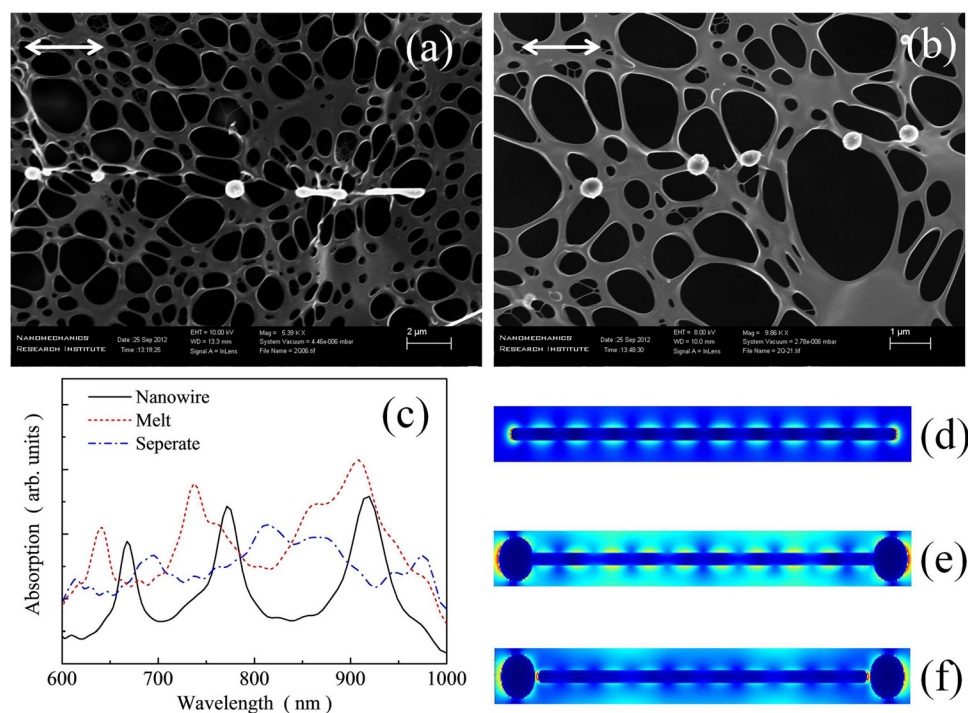


FIG. 3. Laser polarization parallel to the long axis of the Ag nanowire. (a) and (b) After laser-induced melting and separation into nanoparticles and nanobars. (c) Absorption spectra as calculated from FDTD simulation; (d) electric field $|E|$ distribution calculated by FDTD. (e) $|E|$ distribution when the Ag nanorod has melted at both ends. (f) $|E|$ distribution when particles have separated from the end of the nanowire. The arrows indicate the polarization direction.

shifted to the blue (Fig. 3(c)). As heating continues, the quasi-spherical particles at the end of the wire increase in volume and eventually separate from the nanowire forming an air gap between the nanowire and the separated particles (Fig. 3(f)). This gives rise to an additional concentration of the electric field within the resulting air gap. In this case, the absorption spectrum broadens but the amplitude of individual features diminishes. This indicates that the overall absorption increases, but is less wavelength specific once an air gap has formed. The overall effect of this process is to further enhance melting at the ends of the wire until the nanowire finally melts into a number of aligned nanoparticles as seen in Fig. 2(b). Once particles have separated from the end of the wire, the electric field in this region is enhanced even when excited with the weak parallel polarization (1/10) of the elliptically polarized laser beam. This demonstrates that the melting sequence induced by irradiation with parallel and perpendicular polarizations is different, but that in both cases, melting is initiated by the electric field enhancement at the ends of the Ag nanowires.

In conclusion, femtosecond laser radiation has been shown to be a useful tool for the characterization of spatial heating associated with plasmonic excitation in nanostructures. When the resonance wavelength of the nanowire matches that of the incident laser excitation, melting is initiated in regions of strong electric field enhancement. For Ag nanowires this enhancement, together with melting, first occurs at each end of the wire. It is also seen in the junction area between two nanowires. Simulation of the electric field distribution using a FDTD model indicates that the direction of the laser polarization can significantly influence the distribution of plasmonic energy and the evolution of melting. The results of this simulation are in good agreement with experimental observations on the effects of fs laser irradiation on Ag nanowires. This suggests that the unique spatial characteristics associated with plasmonic excitation are potentially useful in the development of new methods of welding, reshaping, and cutting nanowires.

This work was supported by the Canada Research Chairs (CRC) program, by the National Sciences and Engineering

Research Council (NSERC), National Natural Science Foundation of China (Grant No. 51075232), Beijing Natural Science Foundation (Grant No. 3132020), State Key Lab of Advanced Welding & Joining, HIT (No. AWPT-Z12-04), and Tsinghua University Initiative Scientific Research Program (Grant No. 2010THZ 02-1). The authors would like to thank Mr. Fred Pearson from the Canadian Center for Electron Microscopy, McMaster University, for help with TEM. Appreciation is also expressed to Professor Scott Lawson, Dr. Xiaogang Li and Dr. Yuquan Ding from the Centre for Advanced Materials Joining, University of Waterloo for useful discussions.

- ¹J. S. Donner, G. Baffou, D. McCloskey, and R. Quidant, *ACS Nano* **7**, 5457 (2011).
- ²G. L. Liu, J. Kim, Y. Lu, and L. P. Lee, *Nature Mater.* **5**, 27 (2006).
- ³E. B. Dickerson, E. C. Dreaden, X. Huang, I. H. El-Sayed, H. Chu, S. Pushpanketh, J. F. McDonald, and M. A. El-Sayed, *Cancer Lett.* **269**, 57 (2008).
- ⁴Y. F. Huang, K. Sefah, S. Bamrungsap, H. T. Chang, and W. Tan, *Langmuir* **24**, 11860 (2008).
- ⁵E. C. Garnett, W. Cai, J. J. Cha, F. Mahmood, S. T. Connor, M. G. Christoforo, Y. Cui, M. D. McGehee, and M. L. Brongersma, *Nature Mater.* **11**, 241 (2012).
- ⁶A. Hu, P. Peng, H. Alarifi, X. Y. Zhang, J. Y. Guo, Y. Zhou, and W. W. Duley, *J. Laser Appl.* **24**, 042001 (2012).
- ⁷R. F. Oulton, V. J. Sorger, T. Zentgraf, R. M. Ma, C. Gladden, L. Dai, G. Bartal, and X. Zhang, *Nature* **461**, 629 (2009).
- ⁸D. Boyer, P. Tamarat, A. Maali, B. Lounis, and M. Orrit, *Science* **297**, 1160 (2002).
- ⁹S. Berciaud, L. Cognet, G. A. Blab, and B. Lounis, *Phys. Rev. Lett.* **93**, 257402 (2004).
- ¹⁰E. Cubukcu, E. A. Kort, K. B. Crozier, and F. Capasso, *Appl. Phys. Lett.* **89**, 093120 (2006).
- ¹¹N. J. Halas, *Nano Lett.* **10**, 3816 (2010).
- ¹²G. Baffou, M. P. Kreuzer, F. Kulzer, and R. Quidant, *Opt. Express* **17**, 3291 (2009).
- ¹³G. Baffou, R. Quidant, and C. Girard, *Appl. Phys. Lett.* **94**, 153109 (2009).
- ¹⁴G. Baffou and H. Rigneault, *Phys. Rev. B* **84**, 035415 (2011).
- ¹⁵G. Baffou and R. Quidant, "Thermo-plasmonics: using metallic nanostructures as nano-sources of heat," *Laser Photonics Rev.* (published online).
- ¹⁶Z. Wang, K. Kutsukake, H. Kodama, N. Usami, K. Fujiwara, Y. Nose, and K. Nakajima, *J. Cryst. Growth* **310**, 5248 (2008).
- ¹⁷P. Ghenuche, S. Cherukulappurath, T. H. Taminiau, N. F. Van Hulst, and R. Quidant, *Phys. Rev. Lett.* **101**, 116805 (2008).
- ¹⁸D. K. Gramotnev and S. I. Bozhevolnyi, *Nat. Photonics* **4**, 83 (2010).